Cancer Letters 467 (2019) 85–95

Contents lists available at ScienceDirect

Cancer Letters

journal homepage: www.elsevier.com/locate/canlet

Original Articles

CD44(+) tumor cells promote early angiogenesis in head and neck squamous cell carcinoma

Nils Ludwig[a,b,*], Miroslaw J. Szczepanski[c,d], Alicja Gluszko[c], Tomasz Szafarowski[e], Juliana H. Azambuja[a,b,f], Louisa Dolg[g], Nils-Claudius Gellrich[g], Andreas Kampmann[g], Theresa L. Whiteside[a,b,h], Rüdiger M. Zimmerer[g]

[a] Department of Pathology, University of Pittsburgh School of Medicine, Pittsburgh, PA, 15213, USA
[b] UPMC Hillman Cancer Center, Pittsburgh, PA, 15213, USA
[c] Chair and Department of Biochemistry, Medical University of Warsaw, Poland
[d] Department of Otolaryngology, Centre of Postgraduate Medical Education, Warsaw, Poland
[e] Department of Otolaryngology, Faculty of Medicine and Dentistry, Czerniakowski Hospital, Medical University of Warsaw, 19/25 Stępińska Str., 00-739, Warsaw, Poland
[f] Programa de Pós-Graduação Em Biociências, Universidade Federal de Ciências da Saúde de Porto Alegre (UFCSPA), Porto Alegre, RS, Brazil
[g] Department of Oral and Maxillofacial Surgery, Hannover Medical School, Hannover, Germany
[h] Departments of Immunology and Otolaryngology, University of Pittsburgh School of Medicine, Pittsburgh, PA, 15213, USA

ARTICLE INFO

Keywords:
CD44
Angiogenesis
HNSCC
Dorsal skinfold chamber
Head and neck squamous cell carcinoma

ABSTRACT

The role of CD44 in progression of head and neck squamous cell carcinoma (HNSCC) has been controversial. The goal of this study was to study the effects of CD44(+) tumor cells on the initial stages of tumor angiogenesis and to evaluate CD44 as a potential marker of tumor angiogenesis.

The CD44 gene expression was studied using the Cancer Genome Atlas (TCGA) Head and Neck Cancer data base. Expression levels of CD44 and of microvascular density (MVD) markers were assessed by immunohistochemistry performed with tissue microarrays in a cohort of 49 HNSCC patients, 11 patients with dysplasia and 12 control oral mucosa tissues. The 4-nitroquinoline-1-oxide oral carcinogenesis mouse model was used to study CD44 expression during carcinogenesis. Gelatin sponges seeded with CD44(+), CD44(−) and unsorted cancer cells suspended in Matrigel were implanted in NOD/SCID mice into a dorsal skinfold chamber and compared to non-seeded sponges as controls. Angiogenic response was assessed by intravital microscopy.

In the TCGA analysis, CD44 gene expression correlated with various pro-angiogenic genes. In human HNSCC tissues, CD44 expression was upregulated and was associated with blood vessels, although no correlation between MVD and CD44 expression was found. During oral carcinogenesis CD44 expression was upregulated. In dorsal skinfold chambers, CD44(+) cells showed a significantly higher MVD than CD44(−) or unsorted cells ($p < 0.001$).

The results indicate that CD44(+) cells contain pro-angiogenic factors and stimulate tumor angiogenesis in HNSCC. Thus, CD44 might emerge as a potential angiogenic biomarker and a therapeutic target for anti-angiogenic therapies.

1. Introduction

Head and neck squamous cell carcinomas (HNSCCs) are among the most common cancers worldwide, with increasing incidence predominantly in western countries and at younger ages [1]. The 5-year survival rate has improved only marginally in recent decades, which emphasizes the need for advancements in diagnosis, prognosis and treatment of HNSCC [2]. The cell surface-associated glycoprotein, CD44, has been reported to be prominently expressed in several types of cancer, including HNSCC. High grade HNSCCs strongly overexpress CD44, while the CD44 expression on tumor cells differs depending on the anatomical tumor site [3,4]. A meta-analysis of CD44 expression in HNSCC showed that CD44 expression was related to worse T category, N category, tumor grade and prognosis in pharyngeal and laryngeal cancer, while no clear association of CD44 expression and oral cancer progression was observed [5]. In tumors, CD44 is known to participate in numerous cellular functions, including cell proliferation, differentiation, migration, presentation of cytokines, chemokines and growth

* Corresponding author. UPMC Hillman Cancer Center, UPCI Research Pavilion, Suite 1.27, 5117, Centre Avenue, Pittsburgh, PA, 15213.
E-mail address: ludwign@upmc.edu (N. Ludwig).

https://doi.org/10.1016/j.canlet.2019.10.010
Received 20 August 2019; Received in revised form 20 September 2019; Accepted 1 October 2019
0304-3835/

factors and is a receptor for hyaluronic acid [6–8]. Nevertheless, the status of CD44 as a glycoprotein essential for tumor growth remains unclear. In HNSCC, the CD44 phenotype is often referred to as a marker for cancer stem cells (CSCs) [9,10]. The CSC hypothesis considers a small subpopulation of CSCs within the tumor bulk of non-CSCs as a highly effective promoter of tumor progression, chemoresistance and disease recurrence [11]. Independently, CD44(+) cells in HNSCC were found to have properties consistent with those of CSCs [9,12]. However, CD44 overexpression seen in the majority of tumor tissues compromise CD44 as a CSC-specific marker. Instead, the use of multiple markers such as $CD44^{(high)}ALDH^{(high)}CD24^{(low)}$ have been used for the assessment of CSCs in HNSCC [9,12]. CD44(+) cells in primary human HNSCC were also found to have an epithelial-to-mesenchymal (EMT) phenotype and to selectively express the programmed death-ligand 1 (PD-L1) [13].

The formation of new blood vessels is a hallmark of HNSCC progression. The new vessels nourish the tumor by delivering oxygen and nutrients and are indispensable for its growth [14]. Angiogenesis is regulated by a wide spectrum of morphogenic and molecular features as well as numerous pro- and anti-angiogenic factors that contribute to vessel formation and growth [15,16]. In this study, we focus on CD44(+) tumor cells and their role in tumor progression by promoting angiogenesis. In a series of *in vitro* and *in situ* studies with human cells and *in vivo* experiments in two mouse models, we show that CD44(+) tumor cells are directly involved in promoting blood vessel formation. Further, we suggest that CD44 expression levels on HNSCC may serve as a biomarker of early angiogenesis in HNSCC.

2. Material and methods

2.1. The Cancer Genome Atlas (TCGA) analysis

The TCGA Head and Neck Cancer data base was analyzed using the University of California, Santa Cruz (UCSC) Xena Browser [17]. In total, 520 cases of primary HNSCC were included in this study and compared to 44 normal controls. 39 cases of HPV(+) HNSCC and 75 cases of HPV(−) HNSCC were used for further analysis. Angiogenesis-related genes were selected based on a published gene set [18]. Expression heatmaps of defined gene sets were generated and clustered online, and the data were downloaded for subsequent statistical analysis.

2.2. HNSCC patients and tissue microarrays

A retrospective analysis was conducted in 49 HNSCC patients treated by surgery. None of the patients included in this study received radiotherapy or chemotherapy before surgery. The clinical and pathological assessments were based on the TNM and UICC classification systems. Only patients with at least 5 years of follow-up were included in the study. Table S1. lists clinicopathological characteristics of the patient cohort. The follow-up period ranged from 60 to 104 months. The 5-year survival was 45%. Besides the HNSCC group, patients with dysplasia of the epithelium in the upper respiratory tract (n = 11) were also studied. Control specimens consisted of mucus membranes acquired from patients undergoing soft palate surgery due to obstructive sleep apnea (n = 12). All patients were treated at the Department of Otolaryngology, Faculty of Medicine and Dentistry, Medical University of Warsaw (years 2007–2011). The study was approved by the Ethics Committee at the Warsaw Medical University.

Tissue microarrays (TMA) were prepared as previously described using the following antibodies: murine anti-CD44 mAb (1:150, clone DF1485, Dako), murine anti-CD34 Class II mAb (1:50, clone:QBEnd 10, Dako) and murine anti-CD105 mAb (1:25, clone:SN6h, Dako) [19]. Detailed information regarding the determination of CD44 expression and quantification of the microvascular density (MVD) is given in the supplemental experimental procedures.

2.3. The 4-nitroquinoline-1-oxide (4-NQO) oral carcinogenesis model

Twenty female C57BL/6 mice aged 6–8 weeks were purchased from Jackson Laboratories. Protocols for animal experiments were approved by the Institutional Animal Care and Use Committee under the reference number 18042580. To induce the development of oral carcinomas, mice had 4-NQO (Sigma-Aldrich) administered in drinking water at 100 mg/mL for a 16-week period, followed by delivery of normal drinking water thereafter. During this period, tumor incidence was 100%. Mice were monitored 2–3 × per week for weight loss or signs of reduced/altered behavior. The mice were euthanized at 0, 16, 20 and 24 weeks. For tissue histology, oropharyngeal tumors were dissected, placed in 2% paraformaldehyde for 1 h and subsequently in 30% sucrose (Sigma-Aldrich) for 24 h. Samples were embedded in OCT compound (Thermo Fisher Scientific) and stored at −80 °C. Cryostat sections (6 µm) were cut and immunofluorescence staining was performed by incubating sections with a rat anti-mouse CD31 Ab (1:100, clone MEC13.3, BD Biosciences) and a rabbit anti-mouse CD44 Ab (1:100, 550538, clone IM7, BD Biosciences) overnight at 4 °C. After washing, tissue sections were incubated with donkey anti-rat Alexa Fluor 488 or goat anti-rabbit Alexa Fluor 488 Ab (1:500, Invitrogen) for 1 h at RT. Negative controls were stained in parallel using the secondary antibodies alone. Sections were counterstained with Hoechst nuclear stain, mounted and imaged using an Olympus BX51 microscope.

2.4. Cell line and cell culture

The HPV(−) HNSCC cell line TZ291013b was derived from a biopsy of a patient at the Department of Oral and Maxillofacial Surgery, Hannover Medical School as previously described [20]. Institutional Ethics Committee approval was obtained. Cells were used at 9–20 passages. The HPV(−) cell line PCI-30 was established and maintained in our laboratory [21]. The HPV(+) cell lines UMSCC47 and UMSCC90 were established by Dr. Thomas Carey (University of Michigan, Ann Arbor, MI) and were obtained through the courtesy of Robert L. Ferris (UPMC Hillman Cancer Center, Pittsburgh, PA). All cell lines were authenticated prior to their use. Cells were grown in DMEM (Lonza Inc.) supplemented with 1% (v/v) penicillin/streptomycin and 10% (v/v) FBS (Gibco, Thermo Fisher Scientific) at 37 °C and in the atmosphere of 5% CO_2 in air.

2.5. Magnetic-activated cell sorting

Cultured cells were sorted magnetically with a CD44 MicroBead Kit and a MACS Column (Miltenyi Biotec GmbH, Bergisch Gladbach, Germany) according to the manufacturer's protocols. Purity of sorting was validated by flow cytometry. In addition to positive and negative fractions, unsorted cells were analyzed.

2.6. Dorsal skinfold chamber model

Dorsal skinfold chambers were prepared as previously described [20,22–24]. All experiments were approved by the Federal Office for Consumer Protection and Food Safety with the reference number 33.9–42,502–04-11/0401. Female NOD.CB17-*Prkdc*^{scid}/JZtm mice with an age of 4–6 weeks and a body weight of 22–26 g were used for this study and were housed according to the guidelines for immunocompromised rodent husbandry. Detailed information regarding the anesthesia of mice and the surgical preparation of the dorsal skinfold chamber is given in the supplemental experimental procedures.

2.7. Seeding and implantation of porcine gelatin sponges

Gelatin sponges were implanted 3d postoperatively to allow the animals to recover. 1×10^5 magnetically sorted CD44(+) cells (n = 7), CD44(−) cells (n = 8) and unsorted cells (n = 8) deriving from

cultured TZ291013b cells were suspended in 20 μL of growth factor reduced Matrigel® (BD Biosciences), seeded onto a porcine gelatin sponge (Spongostan™, FerrosanMedical Devices A/S, Soeborg, Denmark) and were incubated for 4 h at 37 °C. Mice were anesthetized as described above and the cover glass of the window chamber was temporarily removed. The loaded gelatin sponges were implanted in the chamber and compared to non-seeded gelatin/Matrigel® sponges (n = 7) as control.

2.8. Intravital fluorescence microscopy and image analysis

Intravital fluorescence microscopy (IVM) was performed on the day of cell implantation and 3, 6, and 10 days after implantation, as previously described [20]. Retrobulbar injections of 0.1 mL of 5% (v/v) fluorescein isothiocyanate (FITC)-labeled dextran (Sigma-Aldrich, Taufkirchen, Germany) were performed for contrast enhancement of blood plasma and 0.1 mL of rhodamine 6G (Sigma-Aldrich) was used for the staining of leukocytes. Four ROIs in the border region of the gelatin sponges were captured for an observation period of 20 s using the blue and green filter blocks. A 10 × long distance objective was used for capturing the three-dimensional microvessel structures in eight ROIs at the border zones of the gelatin sponge using the fine drive of the microscope.

Quantitative off-line analysis of recorded data was performed using the CapImage® system (Version 6.02, Zeintl Ing.-Büro, Heidelberg, Germany) as previously reported by our group [20,22,24,25]. In the four ROIs, the diameter, centerline velocity, macromolecular leakage, wall shear rate, volumetric blood flow, and leukocyte-endothelium interaction of the post-capillary and collecting venules were measured. Angiogenesis was quantified by calculating the MVD in cm/cm^2 by dividing the total length of capillaries by the observation area. Detailed information regarding the IVM procedure and the image analysis is given in the supplemental experimental procedures.

2.9. Histology and immunohistochemistry

After the final IVM examination, animals were euthanized and specimens of the dorsal skinfold chamber were fixed in 3.5% (w/v) formaldehyde (Merck KGaA, Darmstadt, Germany) and embedded in paraffin (Leica Biosystems GmbH, Nussloch, Germany). Sections (4 μm) were cut and stained with hematoxylin and eosin (H&E, Merck KGaA). For immunofluorescence staining, sections were incubated with a rabbit anti-mouse CD31 Ab (1:60, Proteintech, Manchester, UK) or a rabbit anti-mouse CD44 Ab (1:100, Acris Antibodies GmbH, Herford, Germany) overnight at 4 °C followed by incubation with the secondary Alexa Fluor® 488 AffiniPure antibody (1:400, Jackson Immuno Research Laboratories, Inc., West Grove, PA, USA). Sections were mounted and counterstained with Roti®-Mount FluorCare DAPI (Carl RothGmbH, Karlsruhe, Germany) and imaged using an Eclipse TE300 microscope (Nikon Corporation, Tokyo, Japan). Stainings for CD44 and CD31 were analyzed by quantifying green fluorescence within the gelatin sponge and adjacent tissue with the ImageJ software (http://rsbweb.nih.gov/ij/). Results were expressed as percentages of positively stained areas within the region of interest (% of ROI).

2.10. Angiogenesis antibody arrays

The relative levels of human angiogenesis–related proteins in CD44(+) and CD44(−) TZ291013b cells were measured using a Human Angiogenesis Array Kit (R&D Systems Inc.) according to the manufacturer's instructions. 200 μg protein isolated from magnetically sorted CD44(+) and CD44(−) TZ291013 cells were added to the array, and the results were analyzed with the ImageJ software.

2.11. Flow cytometry

Cells growing in culture at 80% confluency were suspended in staining buffer (PBS + 3% BSA) and stained with labeled mAbs specific for surface antigens: CD44 (11-0441-82, clone IM7, FITC, eBioscience) and LAP (TGF-β1) (349604, clone TW4-2F8, PE, BioLegend). Isotype control Abs were used in all experiments. Briefly, cells were incubated with mAbs for 30 min in the dark at RT, washed twice in PBS buffer and were analyzed by flow cytometry using an Accuri flow cytometer (BD Bioscience) and the Kaluza 1.5 software.

2.12. Statistical analysis

Statistical analysis of tissue microarray data was performed using the SAS 9.4 software package. Correlations between MVD and CD44 expression were assessed using the Spearman's rank correlation coefficient. Rest of the data were analyzed using GraphPad Prism (v7.0). Results are expressed as means ± SEM (standard error of the mean). Differences between groups were assessed by a one-way ANOVA (analysis of variance). Differences within each group were analyzed by a one-way repeated measurements ANOVA. To isolate differences between pairs of groups, Student-Newman-Keuls post-hoc tests were performed. Differences were considered significant at $p < 0.05$.

3. Results

3.1. CD44 gene expression correlates with expression of pro-angiogenic genes and is upregulated in tumor tissues

The Cancer Genome Atlas (TCGA) was used to study CD44 gene expression in HNSCC patients (n = 520) and to seek evidence for associations of CD44 with the pro-angiogenic genotype. The analysis revealed that HNSCC has the second highest CD44 gene expression among all cancer types included in the Pan-Cancer Atlas (Fig. S1). Compared to solid normal tissue (n = 44), the CD44 gene expression was found to be significantly upregulated in HNSCC ($p < 0.00005$; Fig. 1A). CD44, a receptor for hyaluronic acid, is highly correlated with the gene expression of the three hyaluronan synthases HAS1, HAS2 and HAS3 ($p < 0.00004$, $p = 5.6e\text{-}19$ and $p = 4.9e\text{-}22$, respectively; Fig. 1C). To evaluate the angiogenic potential of the CD44 genes, we searched for correlations of CD44 with a set of 44 genes involved in angiogenesis (see Fig. 1D). 33 genes showed positive correlations with the CD44 gene expression, while 11 were negatively correlated. The positive correlations were significant for 26/33 genes. Importantly, SERPINE1, SERPINB5, PLAU, VEGFC and TGFB1 showed a highly significant correlation with CD44 (Fig. 1D). We then sub-divided the HNSCC patient group into HPV(+) (n = 39) and HPV(−) (n = 75) patients and found higher CD44 gene expression in HPV(−) patients ($p = 1.2 \times 10^{-9}$; Fig. 1B). Although the gene expression levels were lower in the HPV(+) patients, the heatmap, which is presented in Fig. 1E, emphasizes that the correlation of CD44 with pro-angiogenic genes is even stronger in HPV(+) patients with only a few exceptions such as TGFB1, IL1B and MMP8. In order to evaluate whether CD44 expression level is inherited from the origin of the cancer cells or can be considered as an acquired phenotype, we compared the CD44 expression with various stemness markers. Gene expression of THY1, NANOG and POU5F1 was upregulated in cancer tissue compared to solid normal tissue, whereas gene expression of PROM1, CD24, SOX2 and ALDH1A1 was similar or downregulated compared to solid normal tissue (Fig. S2). However, no significant positive correlation was found between the gene expression of these markers and CD44 (Fig. S2), leading to the idea that CD44 expression level can be considered as an acquired phenotype.

CD44 gene expression is, therefore, associated with a pro-angiogenic genotype in HNSCC patients, especially in the HPV(+) patient population.

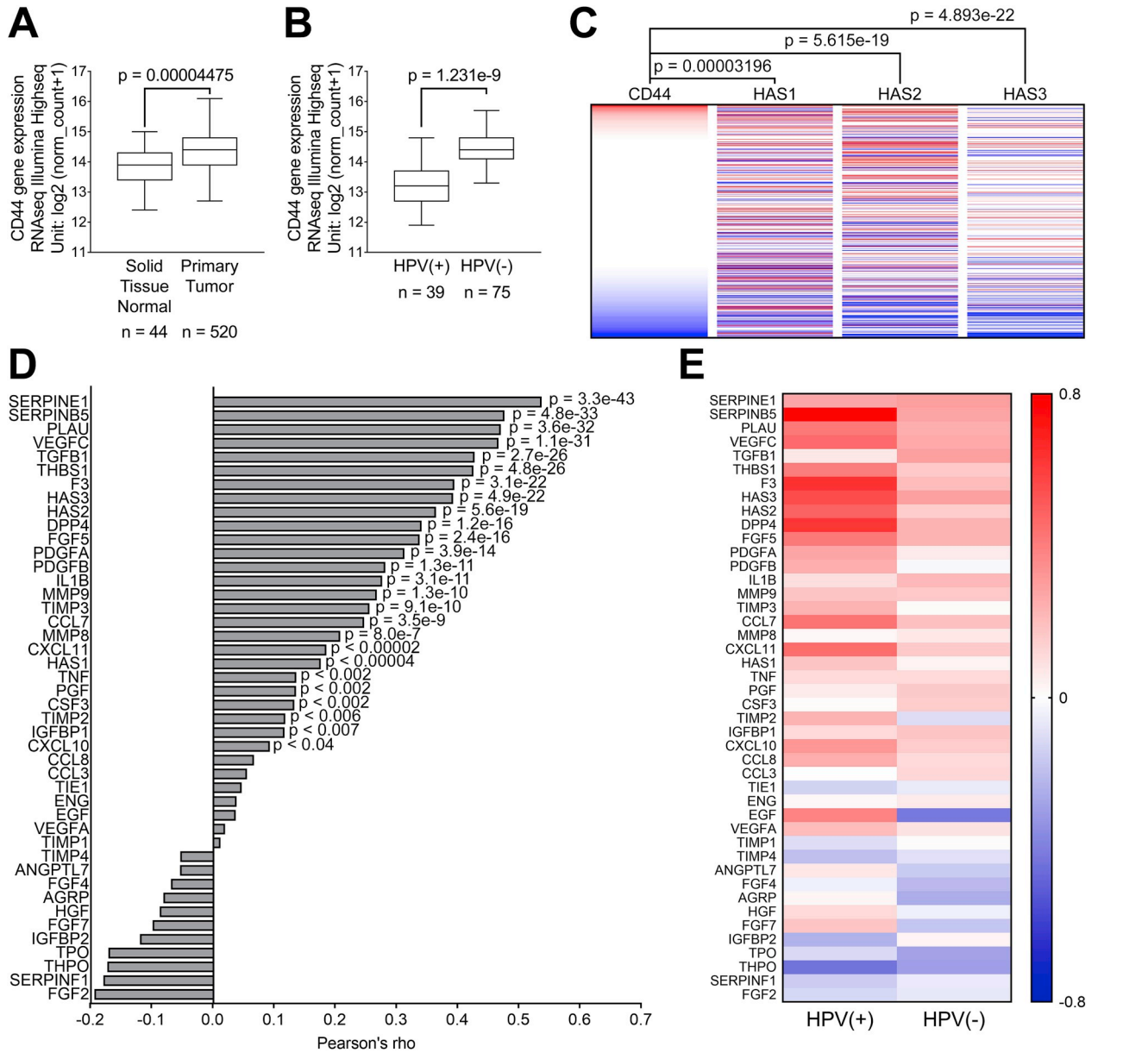

Fig. 1. Analysis of CD44 gene expression in the TCGA data base for HNSCCs using the UCSC Xena Browser. **(A)** Comparison of CD44 gene expression in normal solid tissue and in primary HNSCC tumors. **(B)** Comparison of CD44 gene expression in HPV(+) and HPV(−) HNSCC patients. **(C)** Heat-map from the UCSC Xena Browser based on the primary TCGA HNSCC cohort depicted the gene expression relationship between CD44 and HAS1 (hyaluronan synthase 1), HAS2 (hyaluronan synthase 2) and HAS3 (hyaluronan synthase 3) in 566 patients. **(D)** Correlation of CD44 gene expression with angiogenesis-related genes in TCGA database (n = 566). **(E)** Comparison of correlation of CD44 gene expression with angiogenesis-related genes in HPV(+) (n = 39) and HPV(−) (n = 75) HNSCC patients.

3.2. CD44 correlates with microvascular density in dysplastic lesions

To further validate our findings in the TCGA database at the protein level, IHC staining for CD44 was performed in tissues of 49 HNSCC patients (clinicopathological data are listed in Table S1). We then correlated CD44 expression with the microvascular density (MVD) by staining for the two blood vessel markers, CD105 and CD34. The majority of HNSCC patients overexpressed CD44 (Fig. 2A). Spearman's rank test showed statistically significant ($p = 0.004$) negative correlation between MVD-associated CD34(+) and CD44 expression levels. Negative correlation was also found between MVD-associated CD105(+) and CD44 ($p = 0.005$; Fig. 2B). In control oral mucosa, CD44 expression was low and was not correlated with MVD. In dysplastic mucosa, correlations of CD44 expression with MVD (assessed by CD34 and CD105 staining) showed a weak positive correlation, which was not statistically significant (Fig. 2B). The IHC confirmed the TCGA results, demonstrating significant upregulation of CD44 in tumor tissues compared to normal controls. CD44 was found to be overexpressed in advanced HNSCC. This made the assessment of CD44 expression levels difficult, and contributed to difficulties in establishing correlations between CD44 and CD34 or CD105. In human dysplastic lesions, CD44 expression was lower, allowing for the evaluation of positive correlations with CD34 and CD105. These data suggest that CD44 may be an important marker of early angiogenesis in HNSSC.

3.3. CD44 is upregulated and associates with blood vessels during carcinogenesis

To *in vivo* validate our results obtained with human HNSCC tissues, we used an orthotopic carcinogen-induced mouse model to study the

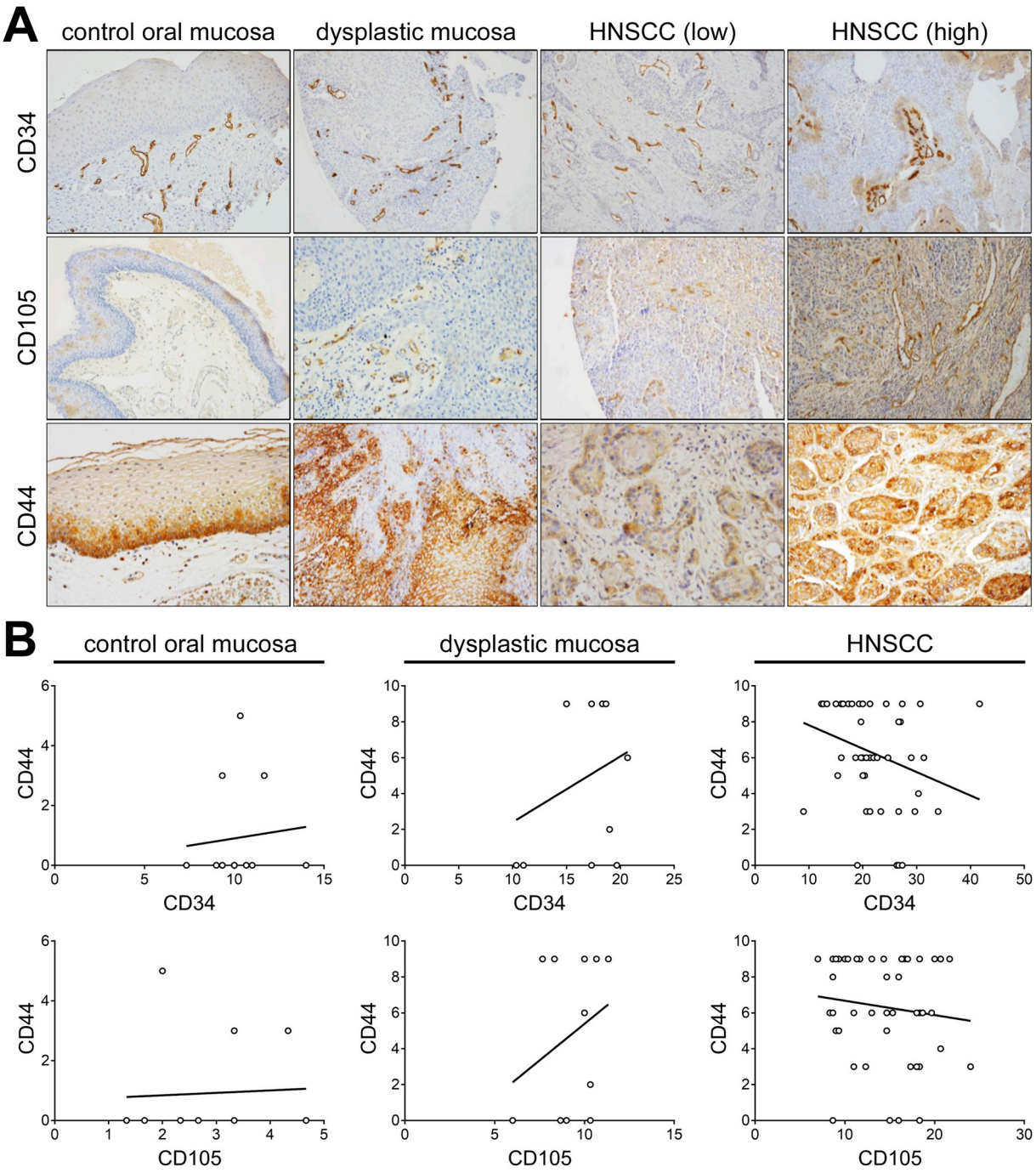

Fig. 2. CD44 expression in HNSCC assessed by immunohistochemistry on tissue microarrays. **(A)** Representative immunohistochemical staining of CD34, CD105 and CD44 in specimen of control oral mucosa, dysplastic mucosa and HNSCC (× 200). For HNSCC patients one representative image with low expression and one representative image with high expression for each marker is shown. **(B)** Correlation of H index of CD44 expression with MVD/CD34 or MVD/CD105 in control oral mucosa, dysplastic mucosa and HNSCC.

CD44 expression at different stages of carcinogenesis. Mice were treated with 4-NQO for 16 weeks and sacrificed at different time points (at 0, 16, 20 and 24 weeks after initial 4-NQO administration). After 16 weeks of 4-NQO administration, mice developed dysplastic tongue lesions, which progressed to early carcinomas at week 20 and advanced carcinomas at week 24. Immunofluorescence staining showed that CD44 was only expressed on mature epithelial cells in healthy tissues, but was subsequently upregulated during tumor progression (Fig. 3A). In healthy tissues, the CD44(+) cells were not localized close to blood vessels (see CD44/CD31 double staining). As soon as dysplastic lesions were present, a close association of CD44(+) cells and blood vessels was observed in the 4-NQO model. The representative immunofluorescence images in Fig. 3A demonstrate that CD44(+) cells are closely associated with the perivascular niche. To validate this observation in human tissues, we performed the same staining on human carcinomas and found a similar staining pattern (Fig. 3B). Interestingly, and unlike staining in the 4-NQO model, CD44(+) cells which were located close to blood vessels co-expressed CD44 and CD31. Thus, CD44(+) cells were present in the perivascular niche in the mouse as well as human tissues and the CD44 expression levels increased during tumor progression.

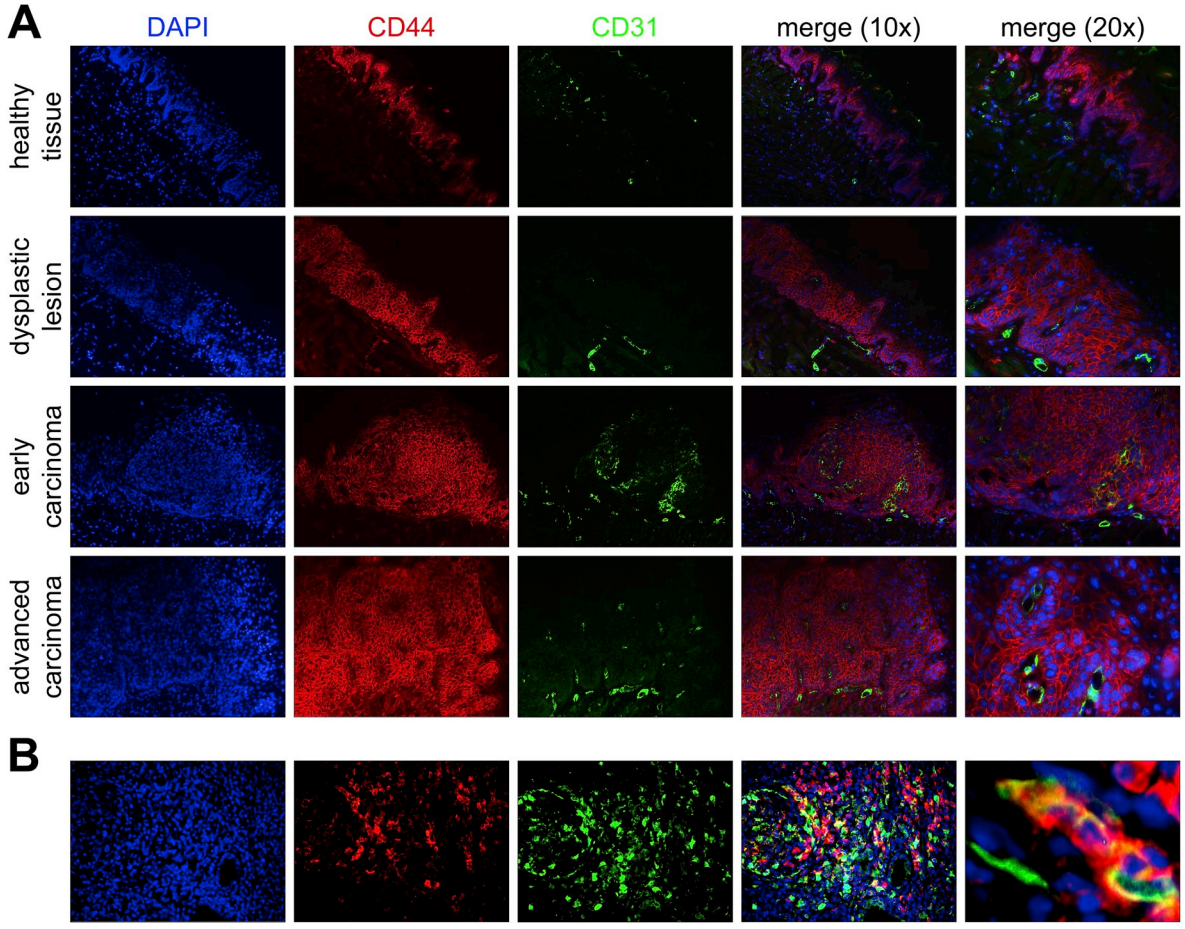

Fig. 3. CD44 expression during carcinogenesis in 4-NQO-treated mice. **(A)** Representative images of sections of 4-NQO oral carcinogenesis. The images show immunofluorescence staining for CD44 (red fluorescence) and CD31 (green fluorescence) with DAPI counterstaining (blue fluorescence) at 10x or 20x magnification as indicated. **(B)** Equivalent staining on human HNSCC tissue. (For interpretation of the references to color in this figure legend, the reader is referred to the Web version of this article.)

3.4. CD44(+) cells induce early angiogenesis in the dorsal skinfold chamber model

The dorsal skinfold chamber mouse model for assessing the capability of CD44(+) cells to induce early angiogenesis *in vivo* was first validated. The dorsal skinfold chamber model is presented in Fig. 4. The diameter of the analyzed postcapillary and collecting venules showed a range from 25.0 to 29.5 µm with no statistical differences and remained constant throughout the observation period (Table S3). To exclude systemic influence on angiogenesis, we determined the centerline velocity (Table S2) and calculated the volumetric blood flow (Table 1). Both parameters remained constant throughout the observation period and showed no significant deviations between the groups. The leukocyte-endothelium interaction can be hindered by increased values of the wall shear rate. The calculation determined constant values in the control and CD44(−) group with no detectable significant differences. Wall shear rate values of the CD44(+) group were increased on day 3 compared to control and on day 6 compared to the CD44(−) group ($p < 0.05$). The implantation of unsorted cells led to constant values till day 6, and a significant increased wall shear rate on day 10 compared to the control group (Table 1).

Next, leukocyte-endothelium interactions and macromolecular leakage were evaluated. Leukocytes were visualized by rhodamine 6G staining and analyzed in post-capillary and collecting venules at the periphery of the gelatin sponges (Fig. 4E). After implantation of cell-seeded gelatin sponges rolling and adherent leukocyte numbers were elevated in all experimental groups compared to control sponges. However, values of the rolling leukocytes showed no statistical differences (Fig. S3A). Mice with implanted CD44(+) cell-seeded sponges had increased numbers of adherent leukocytes on days 3 and 6 compared to controls ($p < 0.05$). Significantly increased values compared to control were also found for CD44(−) cell-seeded sponges on day 6 and sponges seeded with unsorted cells on day 10 (Fig. S3B). The crossing of macromolecules through the endothelial barrier was measured by quantifying the extravasation of FITC-labeled dextran. We encountered a trend of a time-dependent increase of the macromolecular leakage for all groups besides the group with unsorted cells, which shows only a small increase from day 6 to day 10 (Fig. 5C). CD44(+) cell-seeded sponges significantly enhanced the leakage of surrounding vasculature from day 6 to day 10 ($p < 0.05$).

Angiogenic response was also evaluated. To determine differences in the angiogenic potential of the implanted sponges seeded with separated tumor cell subpopulations, angiogenesis was quantified in repeated measurements by calculating the MVD. The contrast enhancement of the blood plasma by FITC-labeled dextran indicated the formation of new vessels 3 days after cell implantation in all groups with cell-seeded sponges. Vessel sprouts originated mostly from the postcapillary and collective venules and a proceeding perfusion of sprouts was observed throughout the observation period. Newly formed microvessels had a heterogeneous appearance with tortuous and twisting sprouts, and disorganized branching. Sponges with CD44(+) cells showed the highest MVD values on all days compared to all other groups ($p < 0.001$). MVD was also enhanced for sponges with CD44(−) or unsorted cells throughout the observation period

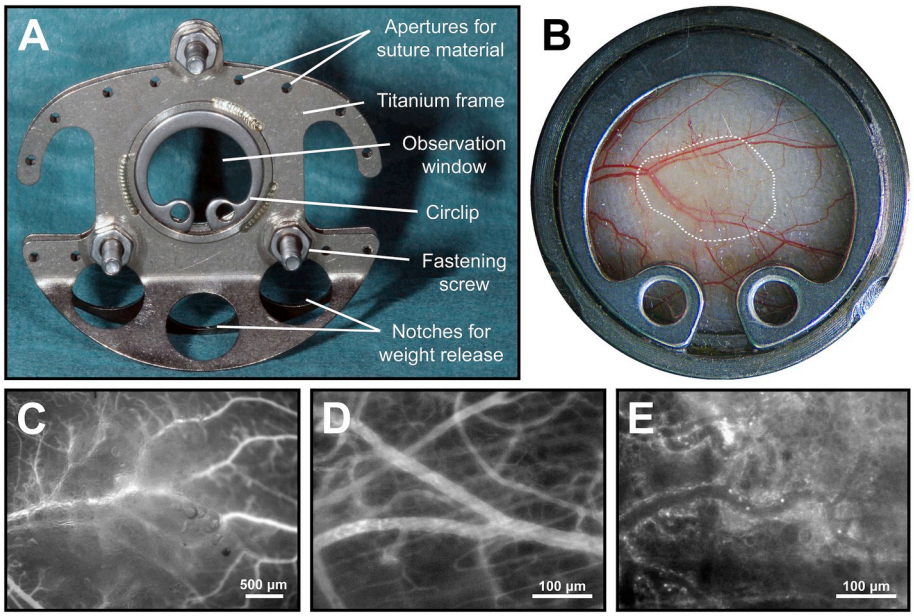

Fig. 4. Demonstration of the dorsal skinfold chamber model. **(A)** The dorsal skinfold chamber consists of two symmetrical titanium frames connected via screws. The observation window (⌀12 mm) is covered with a cover slip and secured with a circlip. **(B)** Overview of the observation window directly after implantation of the cell-seeded gelatin sponge macroscopically and **(C)** magnified by IVM. The sponges are circled by white dots. **(D)** IVM image of a postcapillary venule after contrast enhancement of plasma with FITC-labeled dextran and **(E)** leukocytes stained with rhodamine 6G.

Table 1
Microhemodynamics in postcapillary and collecting venules.[a].

	Day 0	Day 3	Day 6	Day 10
Volumetric blood flow (pl/s)				
control	146.7 ± 30.3	118.0 ± 25.5	178.8 ± 35.3	132.5 ± 23.8
CD44(+)	161.8 ± 27.0	175.9 ± 25.6	184.6 ± 25.8	149.6 ± 28.6
CD44(−)	183.0 ± 23.9	175.7 ± 37.2	155.5 ± 17.8	199.3 ± 40.2
unsorted	146.9 ± 33.1	187.5 ± 40.1	189.6 ± 35.1	148.2 ± 24.4
Wall shear rate (s^{-1})				
control	110.0 ± 17.9	117.0 ± 15.5	125.8 ± 22.0	100.6 ± 9.3
CD44(+)	109.7 ± 8.0	172.5 ± 14.1*	163.6 ± 12.7^{+}	110.2 ± 16.0
CD44(−)	114.3 ± 5.4	111.3 ± 13.1	118.2 ± 11.1	142.8 ± 10.3
unsorted	119.2 ± 17.9	123.0 ± 20.1	142.8 ± 10.4	148.1 ± 13.7*

[a] Volumetric blood flow in pl/s and wall shear rates in s^{-1} of postcapillary and collecting venules at the border zones of the implanted gelatin sponge immediately (day 0) and 3, 6, and 10 days after implantation into the dorsal skinfold chamber of NOD/SCID mice. Values are expressed as means ± SEM; *$p < 0.05$ vs. control on the same day; $^{+}p < 0.05$ vs. CD44(−) on the same day.

compared to the sponges without cells ($p < 0.05$). Unsorted cells promoted a higher angiogenic response compared to the CD44(−) group on all days (Fig. 5B). Fig. 5A highlights our results by showing representative images of IVM 10 days after cell implantation.

3.5. Histologic validation of the model

After the final IVM examination, sections of the dorsal skinfold chambers were H&E-stained to confirm an adequate chamber preparation and to visualize the sponge and adjacent soft tissues. This examination showed that the gelatin sponges were located directly on the musculus panniculus carnosus and confirmed a successful chamber preparation (Fig. 5F). Immunofluorescence staining was performed to determine the phenotype of the isolated subpopulations. Signals for CD44 were not present in the control sponges and in sponges with implanted CD44(−) cells. As expected, CD44(+) cell-seeded sponges showed the highest levels of CD44 signals, followed by the group with unsorted cells ($p < 0.05$ compared to control; Fig. 5D). The MVD values, which were measured by IVM, were confirmed by immunofluorescence staining for CD31. All groups showed positive signals in the muscle tissue and the subcutis located under the gelatin sponge. However, only CD44(+) cells revealed statistical significant results (Fig. 5E).

3.6. CD44(+) subpopulation is enriched in angiogenic factors

To characterize the molecular content of the CD44(+) and CD44(−) cells, which were implanted into the dorsal skinfold chamber, angiogenesis arrays were used. Loading 200 µg of protein derived from CD44(+) and CD44(−) cells revealed that the positive population was enriched in angiogenic factors (Fig. 6A). Largest differences were found for Amphiregulin, Endoglin, Serpin E1 and uPA (Fig. 6B). Different exposure times of the membranes are shown in Fig. S4. To validate these results, we used HNSCC cell lines (PCI-30, UMSCC47 and UMSCC90) and performed flow cytometry to quantify expression levels of LAP (TGF-β1) within the CD44(+) and CD44(−) cell populations. All the investigated cell lines showed an enrichment of LAP within the CD44(+) population (Fig. 6C). Our results demonstrate that the CD44(+) subpopulation is enriched in angiogenic factors.

4. Discussion

This study demonstrates that CD44(+) HNSCC cells have an important impact on the tumor angiogenesis. On the gene level, CD44 expression in HNSCC is the highest relative to multiple other types of cancer, suggesting that CD44 plays an important role in HNSCC. CD44 gene expression is upregulated in HNSCC compared to normal tissues and is highly correlated with pro-angiogenic genes. Most patients included in this study overexpressed CD44, resulting in the highest possible IHC scores. Only 4/49 patients showed no CD44 expression. Similar findings were made in the 4-NQO mouse model. CD44 was overexpressed in all investigated mice with early and advanced tumors, and almost 100% of all tumor cells were positive for CD44. In the HNSCC cell lines, CD44(+) cells represented 80–97% of all cells, depending on the confluency of the culture. These results indicate, that CD44 is a major marker for HNSCC.

In the HNSCC cell lines we studied, CD44(+) cell subpopulations were enriched in pro-angiogenic factors and stimulated early angiogenesis *in vivo* in only 3 days. IHC of HNSCC tissues did not reveal correlations of CD44 expression levels and MVD. In contrast, dysplastic lesions showed a positive correlation. This suggests that the time of cancer progression is critical for demonstrating the pro-angiogenic effects of CD44(+) cells. Possibly, the initial formation of blood vessels is stimulated by CD44(+) cells, but uniformly strong CD44 overexpression in advanced carcinomas might mask the actual pro-angiogenic capacity of CD44.

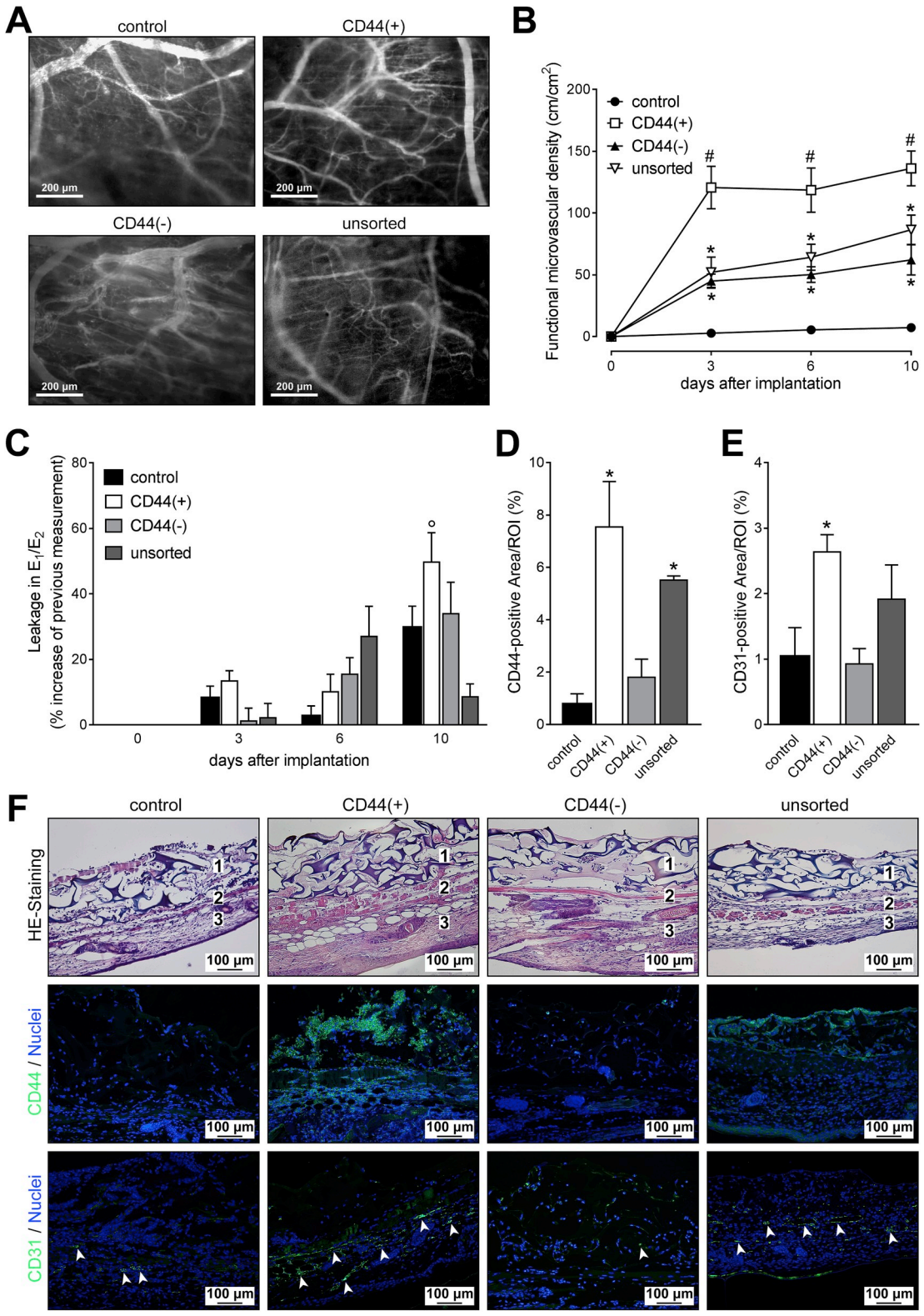

Fig. 5. Angiogenic response to implanted CD44(+) cells in dorsal skinfold chamber model. **(A)** Representative IVM images taken at 10 days after implantation. **(B)** Microvascular density (MVD) of newly formed microvessels, in regions of interest, expressed in units of cm/cm^2 immediately (day 0) and 3, 6, and 10 days after implantation of the gelatin sponges into dorsal skinfold chambers in NOD/SCID mice. **(C)** Macromolecular leakage as an indicator of microvascular permeability expressed as percent increase compared to previous measurement. **(D)** Quantitative analysis of CD44(+) and **(E)** CD31(+) signals by immunofluorescent staining. Data in D and E are expressed as the percentage of the area that was positively stained from the region of interest (% ROI). **(F)** Representative histological stainings of the dorsal skinfold chamber 10 days after implantation of gelatin sponges in 20x magnification. HE-Staining (1: Matrigel®/gelatin sponge. 2: musculus panniculus carnosus. 3: subcutis). Immunofluorescence staining for the detection of CD44(+) cells or CD31(+) cells (green fluorescence). White arrows: Endothelial structures. Sections were counterstained with DAPI (blue fluorescence). All values represent means ± SEM; $^*p < 0.05$ vs. the control group on the same day; $^\#p < 0.001$ vs. any other group on the same day; $^\circ p < 0.05$ vs. the same group on the previous day. (For interpretation of the references to color in this figure legend, the reader is referred to the Web version of this article.)

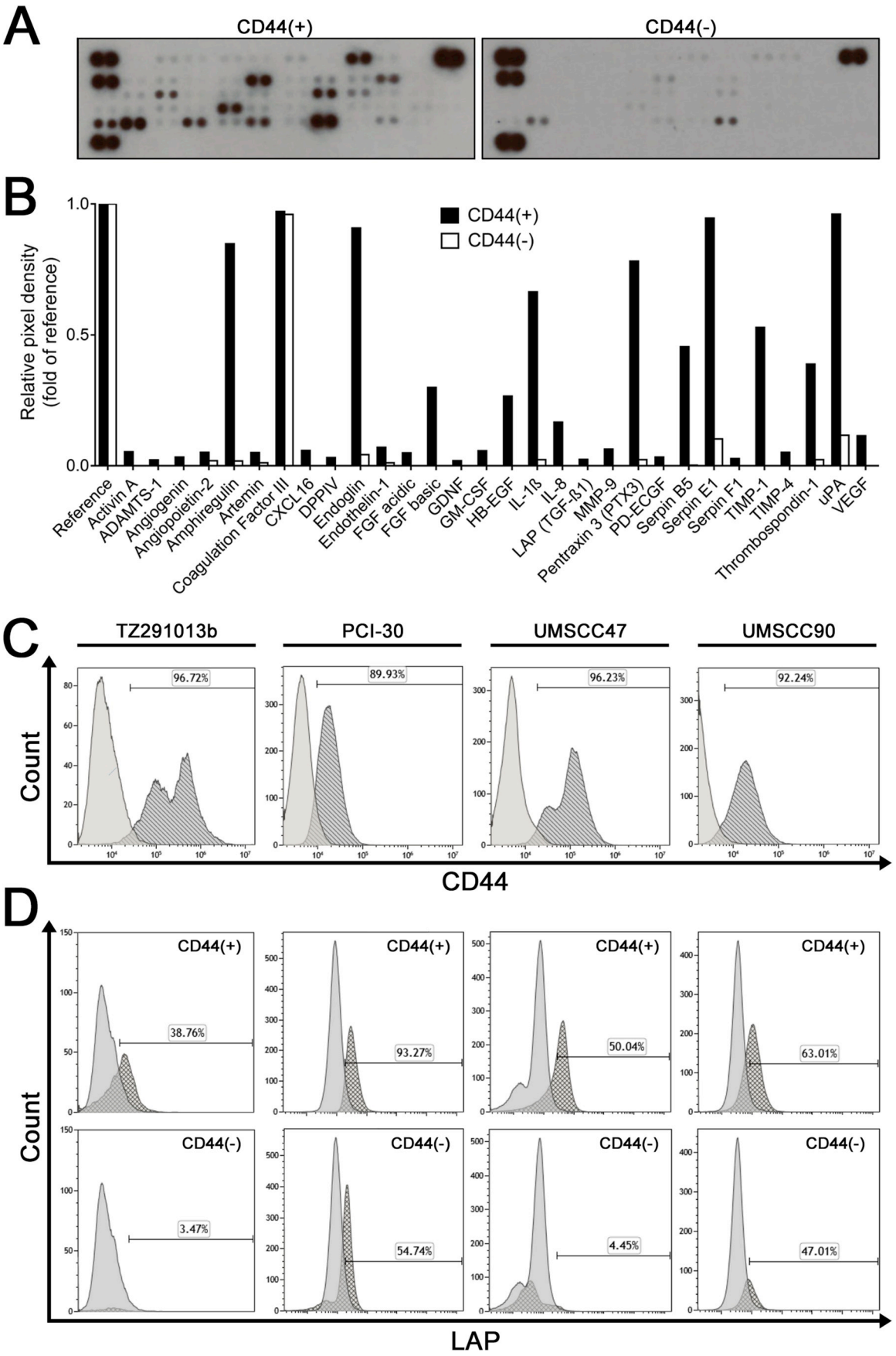

Fig. 6. The angiogenesis antibody arrays **(A)** show the analysis of 200 μg total protein of CD44(+) cell lysate (left array) and CD44(−) cell lysate (right array) regarding their molecular content. The arrays were quantified in **(B)** using ImageJ. Values are normalized to reference spots on the membranes (top left, top right, and bottom left). **(C)** CD44 expression by TZ291013b, PCI-30, UMSCC47 and UMSCC90 cells (left to right). **(D)** Multicolor flow cytometry for CD44 and LAP. Histograms show LAP expression within the CD44(+) or CD44(−) population for TZ291013b, PCI-30, UMSCC47 and UMSCC90 cells (left to right).

It was previously reported, that CD44(+) HNSCC stem cells actively interact with surrounding stroma cells in the tumor microenvironment. The cells coopt pre-existing vessels and use the perivascular niche for their survival [26]. We observed that CD44(+) cells are localized in the perivascular niche in the mouse as well as in human tumor tissues. The self-renewal and growth of CD44(+) cells in the perivascular niche is stimulated by factors released by the surrounding endothelial cells, as reported previously [26]. It is, therefore, possible, that the CD44(+) cell subpopulation is enriched in cells with CSC features, which promote neovascularization. The migration of endothelial progenitor cells (EPCs) towards the tumor site is promoted by proangiogenic factors produced by CSCs [27,28]. CSCs also have the capability to differentiate into endothelial cells and to be incorporated in newly forming vessels [29]. Recently, we used the dorsal skinfold chamber model for the implantation of CD133(+) melanoma CSCs to show the angiogenic potential of cells with the CSC phenotype [30]. The implantation of CD44(+) HNSCC cells in this study was similar to our earlier results.

This study suggests that targeting CD44 in HNSCC, might decrease vascularization and tumor progression. Since the CD44(+) subpopulation might be enriched in CSCs, the targeting of CD44 might overcome the commonly observed chemoresistance of CSCs and limit their survival of CSCs. The literature suggests several ways amenable to targeting CD44. Humanized antibodies have already been used in clinical trials for treatment of HNSCC, but since CD44 is also expressed in healthy tissues, resulting in off-target effects [31]. Instead of targeting CD44, it might be possible to target CD44v6, a CD44 isoform, which is considered to be more tumor specific [31]. Pharmacological approaches to inhibition of CD44 were also introduced, especially Silibinin [32]. In addition, direct targeting of CD44/hyaluronic acid interactions might be promising for reducing CD44-mediated effects as well as downregulating CD44 [31,33]. However, these approaches have to be carefully investigated and compared in their efficacy for improving disease outcome and progression. The assessment of an indvidual risk profile including the CD44 expression as well as the tissue vascularization in early tumors might justify the use of CD44 as a target.

5. Conclusion

This study emphasizes the importance of CD44 as a potential early marker of angiogenesis as well as an important modulator for the dynamic process of angiogenesis. CD44 emerges as a useful target in HNSCC since it is overexpressed in most carcinomas. Especially the targeting of CD44 with antibodies, peptides or pharmacological inhibition in early stage tumors might decrease neovascularization and might, therefore, be beneficial in reducing tumor progression.

Declaration of competing interest

No potential conflict of interest was reported by the authors.

Acknowledgments

N.L. was supported by the Leopoldina Fellowship LPDS 2017–12 from German National Academy of Sciences Leopoldina. The research group at the Department of Oral and Maxillofacial Surgery, Hannover Medical School was supported by the Cancer Society of Lower Saxony (Niedersächsische Krebsgesellschaft e.V.). The study was partially funded from the National Science Center, Poland 2017/26/M/NZ5/00877# to M.J.S., J.H.A. was supported by the Programa de Doutorado Sanduíche no Exterior (PDSE) 88881.188926/2018–01 from Coordenação de Aperfeiçoamento de Pessoal de Nível Superior (CAPES).

Appendix A. Supplementary data

Supplementary data to this article can be found online at https://doi.org/10.1016/j.canlet.2019.10.010.

References

[1] A.K. Chaturvedi, W.F. Anderson, J. Lortet-Tieulent, M. Paula Curado, J. Ferlay, S. Franceschi, P.S. Rosenberg, F. Bray, M.L. Gillison, Worldwide trends in incidence rates for oral cavity and oropharyngeal cancers, J. Clin. Oncol. 31 (2013) 4550–4559.
[2] C.K. Howlader N, A.M. Noone, M. Krapcho, J. Garshell, D. Miller, S.F. Altekruse, C.L. Kosary, M. Yu, J. Ruhl, Z. Tatalovich, A. Mariotto, D.R. Lewis, H.S. Chen, E.J. Feuer, SEER Cancer Statistics Review, 1975-2011, Natl. Cancer Institute., Bethesda, MD, 2013.
[3] P. Shakib, F. Ensani, A. Abdirad, B. Valizadeh, M. Seyedmajidi, S. Sum, CD44 and CD74: the promising candidates for molecular targeted therapy in oral squamous cell carcinoma, Dent. Res. J. 12 (2015) 181–186.
[4] M. Krump, J. Ehrmann, Differences in CD44s expression in HNSCC tumours of different areas within the oral cavity, Biomed. Pap. 157 (2013) 280–283, https://doi.org/10.5507/bp.2012.107.
[5] J. Chen, J. Zhou, J. Lu, H. Xiong, X. Shi, L. Gong, Significance of CD44 expression in head and neck cancer: a systemic review and meta-analysis, BMC Canc. 14 (2014) 1–9.
[6] D. Naor, S. Nedvetzki, I. Golan, L. Melnik, Y. Faitelson, CD44 in cancer, Crit. Rev. Clin. Lab. Sci. 39 (2008) 527–579.
[7] D. Assimakopoulos, E. Kolettas, G. Patrikakos, A. Evangelou, The role of CD44 in the development and prognosis of head and neck squamous cell carcinomas, Histol. Histopathol. 17 (2002) 1269–1281.
[8] A. Shah, S. Patel, J. Pathak, N. Swain, S. Kumar, The evolving concepts of cancer stem cells in head and neck squamous cell carcinoma, Sci. World J. 2014 (2014).
[9] S. Ghuwalewala, D. Ghatak, P. Das, S. Dey, S. Sarkar, N. Alam, C.K. Panda, S. Roychoudhury, CD44highCD24low molecular signature determines the cancer stem cell and EMT phenotype in oral squamous cell carcinoma, Stem Cell Res. 16 (2016) 405–417.
[10] P.S. Satpute, V. Hazarey, R. Ahmed, L. Yadav, Cancer stem cells in head and neck squamous cell carcinoma: a review, Asian Pac. J. Cancer Prev. APJCP 14 (2013) 5579–5587.
[11] M.E.P. Prince, L.E. Ailles, Cancer stem cells in head and neck squamous cell cancer, J. Clin. Oncol. 26 (2008) 2871–2875.
[12] J. Han, T. Fujisawa, S.R. Husain, R.K. Puri, Identification and characterization of cancer stem cells in human head and neck squamous cell carcinoma, BMC Canc. 14 (2014) 173.
[13] Y. Lee, J.H. Shin, M. Longmire, H. Wang, H.E. Kohrt, H.Y. Chang, J.B. Sunwoo, Cd44+ cells in head and neck squamous cell carcinoma suppress t-cell-mediated immunity by selective constitutive and inducible expression of PD-L1, Clin. Cancer Res. 22 (2016) 3571–3581, https://doi.org/10.1158/1078-0432.CCR-15-2665.
[14] N. Ludwig, S.S. Yerneni, B.M. Razzo, T.L. Whiteside, Exosomes from HNSCC promote angiogenesis through reprogramming of endothelial cells, Mol. Cancer Res. 16 (2018) 1798–1808.
[15] B. Döme, M.J.C. Hendrix, S. Paku, J. Tóvári, J. Tímár, Alternative vascularization mechanisms in cancer: pathology and therapeutic implications, Am. J. Pathol. 170 (2007) 1–15.
[16] P. Carmeliet, R.K. Jain, Angiogenesis in cancer and other diseases, Nature 407 (2000) 249–257.
[17] M. Goldman, B. Craft, A. Kamath, A. Brooks, J. Zhu, D. Haussler, The UCSC Xena Platform for Cancer Genomics Data Visualization and Interpretation, (2018), p. 326470 bioRxiv.
[18] C.-L. Kuo, A wide-spectrum analysis of angiogenesis-related factors in ovarian cancer reveals a signature potentially for prognosis and therapeutic targeting, Cancer Res. 78 (2018) 16 LP-16.
[19] T. Szafarowski, J. Sierdzinski, M.J. Szczepanski, T.L. Whiteside, N. Ludwig, A. Krzeski, Microvessel density in head and neck squamous cell carcinoma, Eur. Arch. Oto-Rhino-Laryngol. 275 (7) (2018) 1845–1851.
[20] R.M. Zimmerer, N. Ludwig, A. Kampmann, G. Bittermann, S. Spalthoff, M. Jungheim, N.-C. Gellrich, F. Tavassol, CD24 + tumor-initiating cells from oral squamous cell carcinoma induce initial angiogenesis in vivo, Microvasc. Res. 112 (2017) 101–108.
[21] D.S. Heo, C. Snyderman, S.M. Gollin, S. Pan, E. Walker, R. Deka, E.L. Barnes, J.T. Johnson, R.B. Herberman, Biology, cytogenetics, and sensitivity to immunological effector cells of new head and neck squamous cell carcinoma lines, Cancer Res. 49 (1989) 5167–5175.
[22] M. Rücker, M.W. Laschke, D. Junker, C. Carvalho, F. Tavassol, R. Mülhaupt, N.C. Gellrich, M.D. Menger, Vascularization and biocompatibility of scaffolds consisting of different calcium phosphate compounds, J. Biomed. Mater. Res. A 86 (2008) 1002–1011.
[23] F. Tavassol, P. Schumann, D. Lindhorst, B. Sinikovic, A. Voss, C. von See, A. Kampmann, K. Bormann, C. Carvalho, R. Mülhaupt, Y. Harder, M. Laschke, M. Menger, N. Gellrich, M. Rücker, Accelerated angiogenic host tissue response to poly(L-lactide-co-glycolide) scaffolds by vitalization with osteoblast-like cells, Tissue Eng. A 16 (2010) 2265–2269.
[24] A. Kampmann, D. Lindhorst, P. Schumann, R. Zimmerer, H. Kokemüller, M. Rücker, N.C. Gellrich, F. Tavassol, Additive effect of mesenchymal stem cells and VEGF to vascularization of PLGA scaffolds, Microvasc. Res. 90 (2013) 71–79.
[25] S. Gniesmer, R. Brehm, A. Hoffmann, D. Cassan, H. Menzel, A. Hoheisel, B. Glasmacher, E. Willbold, J. Reifenrath, M. Wellmann, N. Ludwig, F. Tavassol, R. Zimmerer, N. Gellrich, A. Kampmann, In vivo analysis of vascularization and biocompatibility of electrospun polycaprolactone fiber mats in the rat femur chamber, J. Tissue Eng. Regenerat. Med. (2019) 1–13.
[26] S. Krishnamurthy, Z. Dong, D. Vodopyanov, A. Imai, J.I. Helman, M.E. Prince,

M.S. Wicha, J.E. Nor, Endothelial cell-initiated signaling promotes the survival and self-renewal of cancer stem cells, Cancer Res. 70 (2010) 9969–9978.
[27] S. Kaur, P. Bajwa, A "tête-à tête" between cancer stem cells and endothelial progenitor cells in tumor angiogenesis, Clin. Transl. Oncol. 16 (2014) 115–121.
[28] L. Treps, R. Perret, S. Edmond, D. Ricard, J. Gavard, Glioblastoma stem-like cells secrete the pro-angiogenic VEGF-A factor in extracellular vesicles, J. Extracell. Vesicles 6 (2017) 1359479.
[29] P. Carmeliet, R.K. Jain, Molecular mechanisms and clinical applications of angiogenesis, Nature 473 (2011) 298–307.
[30] R.M. Zimmerer, P. Matthiesen, F. Kreher, A. Kampmann, S. Spalthoff, P. Jehn, G. Bittermann, N.C. Gellrich, F. Tavassol, Putative CD133+ melanoma cancer stem cells induce initial angiogenesis in vivo, Microvasc. Res. 104 (2016) 46–54.
[31] C. Chen, S. Zhao, A. Karnad, J.W. Freeman, The biology and role of CD44 in cancer progression: therapeutic implications, J. Hematol. Oncol. 11 (2018) 1–23.
[32] A.M. Handorean, K. Yang, E.W. Robbins, T.W. Flaig, K.A. Iczkowski, Silibinin suppresses CD44 expression in prostate cancer cells, Am. J. Transl. Res. 1 (2009) 80–86.
[33] J. Zheng, S. Zhao, X. Yu, S. Huang, H.Y. Liu, Simultaneous targeting of CD44 and EpCAM with a bispecific aptamer effectively inhibits intraperitoneal ovarian cancer growth, Theranostics 7 (2017) 1373–1388.